ACS Catalysis

Perspective

pubs.acs.org/acscatalysis

Heteroatom-Doped Graphitic Carbon Catalysts for Efficient Electrocatalysis of Oxygen Reduction Reaction

Jintao Zhang[†] and Liming Dai*

Center of Advanced Science and Engineering for Carbon (Case4carbon), Department of Macromolecular Science and Engineering, Case Western Reserve University, 10900 Euclid Avenue, Cleveland, Ohio 44106, United States

ABSTRACT: The oxygen reduction reaction (ORR) plays an important role in renewable energy technologies, such as fuel cells and metal−air batteries. Along with the extensive research and development of nonprecious metal catalysts (NPMCs) to reduce/replace Pt for electrocatalytic reduction of oxygen, a new class of heteroatom-doped metal-free carbon catalysts has been recently developed, which, as alternative ORR catalysts, could dramatically reduce the cost and increase the efficiency of fuel cells and metal−air batteries. The improved catalytic performance of heteroatom-doped carbon ORR catalysts has been attributed to the doping-induced charge redistribution around the heteroatom dopants, which lowered the ORR potential and changed the O_2 chemisorption mode to effectively weaken the O−O bonding, facilitating ORR at the heteroatom-doped carbon electrodes. Subsequently, this new metal-free ORR mechanism was confirmed by numerous studies, and the same principle has been applied to the development of various other efficient catalysts for not only ORR in fuel cells but also oxygen evolution reaction (OER) in metal−air batteries and hydrogen evolution reaction (HER) in water-splitting systems. However, there are still some concerns about possible contributions of metal impurities to the ORR activities of these carbon catalysts. To avoid unnecessary confusion, therefore, it is important to clarify the situation. In this Perspective, we provide important aspects of the metal-free ORR catalysts with a critical analysis of the literature, along with perspectives and challenges of this rapidly growing field of practical significance.

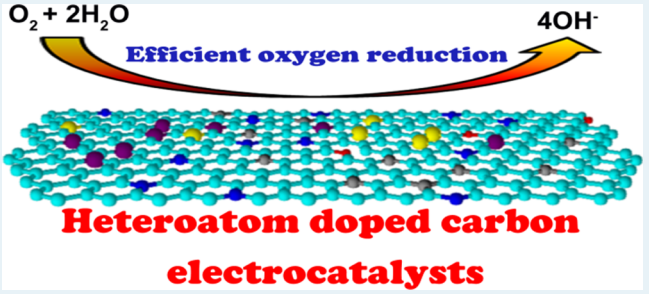

KEYWORDS: *graphitic carbon, heteroatom doping, oxygen reduction reaction, fuel cell, metal−air battery*

1. INTRODUCTION

Oxygen reduction reaction (ORR) plays an important role in renewable energy technologies, ranging from fuel cells to metal−air batteries.[1] ORR involves multiple electrochemical reactions and can proceed either through a two-step, two-electron (2e) pathway with the formation of H_2O_2 (in acidic medium) or HO_2^- (in alkaline media) as the intermediate specie or via a more efficient four-electron (4e) process to reduce O_2 directly into H_2O (in acidic media) or OH^- (in alkaline media) to combine with proton into water (Scheme 1):[2]

Scheme 1. Oxygen Reduction Reaction in Acid and Alkaline Media, Respectively

Acid media: $O_2 + 2H^+ + 2e^- \rightarrow H_2O_2$ (Two electron process)

$H_2O_2 + 2H^+ + 2e^- \rightarrow 2H_2O$

$O_2 + 4H^+ + 4e^- \rightarrow 2H_2O$ (Four electron process)

Alkaline media: $O_2 + H_2O + 2e^- \rightarrow HO_2^- + OH^-$ (Two electron process)

$H_2O + HO_2^- + 2e^- \rightarrow 3OH^-$

$O_2 + 2H_2O + 4e^- \rightarrow 4OH^-$ (Four electron process)

Electrocatalysts are required to lower activation energy barriers of the sluggish ORR, boosting performance of fuel cells and metal−air batteries. Although platinum (Pt) has been long known as the best ORR catalyst, its high cost and scarcity have hampered the large-scale commercialization of fuel cell and metal−air battery technologies.[3] In particular, commercialization of the fuel cell technology has been further limited by the poor operation durability, fuel crossover effect, and CO-poisoning effect intrinsically associated with the Pt catalyst.[1b] Over the past half a century or so, therefore, intensive research efforts have been made to exploit alternative ORR electrocatalysts based on Pt alloys or nonprecious transition metal chalcogenides to reduce or replace Pt.[4] Nonprecious metal oxide catalysts have also been explored as alternative electrocatalysts for ORR.[5] However, the catalytic activity of these nonprecious metal catalysts (NPMCs) often decrease significantly along with the metal leaching during usage, leading to a poor durability.[6]

Along with the extensive research and development of NPMCs, a new class of carbon-based metal-free ORR catalysts has recently been developed.[7] Carbon materials, including

Received: April 1, 2015
Revised: October 21, 2015

DOI: 10.1021/acscatal.5b01563
ACS Catal. 2015, 5, 7244−7253

carbon nanotubes (CNTs), graphene, and porous carbons with unique physicochemical structures, excellent electric/thermal conductivities, and multiple catalytic active sites, are of particular interest as low-cost electrocatalysts for a variety of redox reactions.[8] Doping carbon nanomaterials with heteroatoms (e.g., N, S, B, P) could cause electron modulation to tune their chemical activities.[9] Indeed, recent efforts have led to the development of heteroatom-doped carbon nanomaterials as efficient electrocatalysts for ORR.[9] The improved catalytic performance of heteroatom-doped carbon ORR catalysts has been attributed to the doping-induced charge redistribution around the heteroatom dopants, which changed the O_2 chemisorption mode to effectively weaken the O−O bonding and facilitate the ORR process.[7] Furthermore, recent studies have also led to various carbon-based metal-free catalysts for oxygen evolution reaction (OER), hydrogen evolution reaction (HER), and other reactions.[10] However, there are still some concerns about possible contributions of metal impurities to the ORR activities of these metal-free carbon catalysts.[11] Although the concerns are arising from a couple of groups only, it is important to avoid the unnecessary confusion. Herein, we clarify the situation by providing a brief summary of recent progresses on the rational design and development of heteroatom-doped carbon nanomaterials for efficient ORR electrocatalysis, along with a critical analysis of the relevant literature as well as perspectives and challenges for this exciting field.

2. INTRINSIC CATALYTIC NATURE OF HETEROATOM-DOPED CARBON NANOSTRUCTURES

Nonprecious metal ORR electrocatalysts have been developed from nitrogen- and Co/Fe-containing precursors, including metal porphyrin or phthalocyanine.[13] Recently, NPMCs with carbon-supported, nitrogen-rich metal complexes (M−N_x−C) were produced by high-temperature pyrolysis of various nitrogen-rich (macro)molecules, such as polypyrrole,[13b,c] polyaniline,[14] phenanthroline,[5b] polyimide,[15] and 2,6-diaminopyridine,[16] incorporating iron and cobalt. By either direct pyrolysis of nitrogen-containing precursors or post-treatment of preformed carbon nanomaterials with N-containing species, nitrogen-doping could be achieved, which was demonstrated to be an effective approach for intrinsically tailoring the catalytic activities of carbon nanomaterials.[9f,17] Of particular importance, Gong et al., reported that vertically aligned nitrogen-doped carbon nanotubes (VA-NCNTs) can catalyze a four-electron ORR process free from CO "poisoning" with a much better durability than that of commercially available Pt-based electrodes in alkaline electrolytes (Figure 1a).[7] The high surface area, good electrical and mechanical properties, and superb thermal stability of aligned CNTs provide additional benefits for the nanotube electrode to be used in fuel cells under both ambient and harsh conditions. According to experimental observations and theoretical calculations by B3LYP hybrid density functional theory (DFT), the improved catalytic performance is contributed to the electron-accepting ability of the nitrogen atoms to create a net positive charge on adjacent carbon atoms in the VA-NCNT (Figure 1b), which changes the chemisorption mode of O_2 from the usual end-on adsorption (Pauling model) at the nitrogen-free CNT (CCNT) surface (top, Figure 1c) to a side-on adsorption (Yeager model) onto the NCNT electrode (bottom, Figure 1c).[7] The N-doping-induced charge-transfer from adjacent carbon atoms

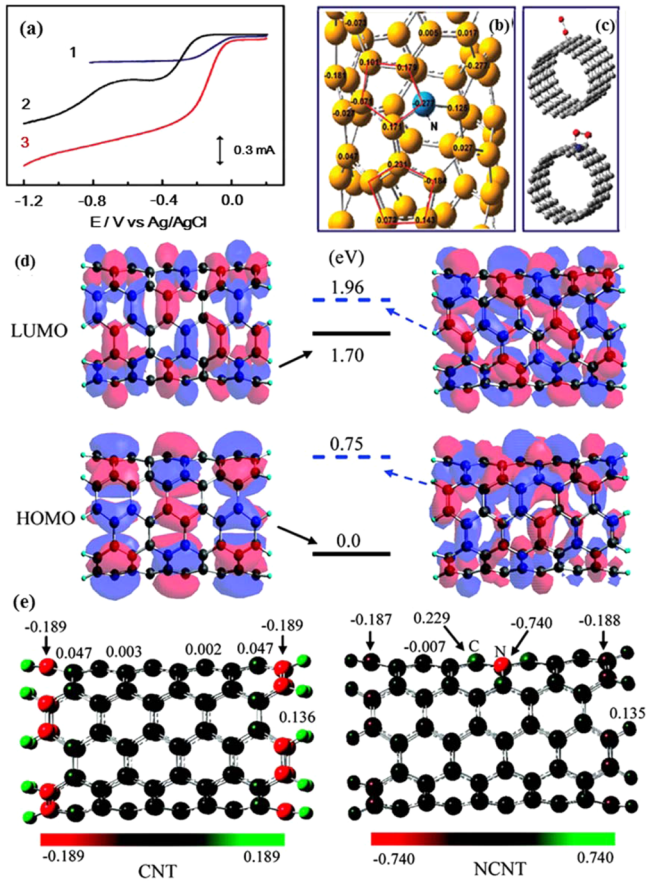

Figure 1. (a) RDE voltammograms for oxygen reduction in air-saturated 0.1 M KOH at the Pt−C/GC (curve 1), VA-CCNT/GC (curve 2), and VA-NCNT (curve 3) electrodes. (b) Calculated charge density distribution for the NCNTs. (c) Schematic representations of possible adsorption modes of an oxygen molecule at the CCNTs (top) and NCNTs (bottom). The C atoms around the pyrrolic-like nitrogen could possess much higher positive charges than do the C atoms around the pyridinic-like nitrogen. Reproduced with permission from ref 7. Copyright 2009 AAAS. (d) LUMO/HOMO and (e) charge distribution of (5,5)-12.9 (length) CNT and NCNT. Reproduced with permission from 19a. Copyright 2010 American Chemical Society.

could lower the ORR potential while the parallel diatomic adsorption could effectively weaken the O−O bonding, facilitating oxygen reduction at the VA-NCNT electrode. This seminal work was followed by many studies, and the diversity of carbon-based metal-free electrocatalysts has since been significantly broadened.[8−10,18]

Subsequent studies revealed that N-doping can reduce the band gap between the highest-occupied molecular orbital (HOMO) and the lowest-unoccupied molecular orbital (LUMO) by lifting the energy level of HOMO (Figure 1d), which facilitates the electron transfer from the N-doped CNT to the adsorbed oxygen.[19] Compared with the undoped CNT, the nitrogen atom on the NCNT shows remarkably high negative charge, whereas the carbon atoms around the nitrogen dopant show significant amounts of positive charge, indicating a doping-induced charge redistribution (Figure 1e). The N-doping-induced electron-deficient carbon atoms enhance the chemsorption of O_2 and hence the observed ORR electrocatalytic activities for NCNTs.

The various nitrogen-doped configurations with different nitrogen environments would affect the electronic structure of

DOI: 10.1021/acscatal.5b01563
ACS Catal. 2015, 5, 7244−7253

neighbor carbon atoms and then lead to different catalytic properties.[20] The edge structure and doped-N near the edge are shown to enhance the oxygen adsorption and the catalytic activity toward ORR. Besides, the armchair and zigzag sites located at the edges via the sp^2 hybridization are high-energy sites which can be functionalized with heteroatoms, providing strong chemical reactivity.[21] It is generally difficult to obtain an unambiguous comparison among the activities of various nitrogen configurations (such as pyrrolic, pyridinic, and graphitic nitrogen in Figure 2).[20a] The pyrrolic and pyridinic

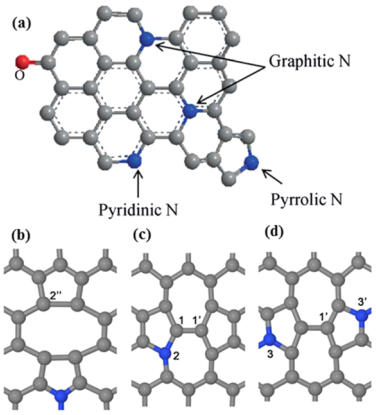

Figure 2. (a) Different forms of nitrogen-functionalized carbon. C gray, N blue, and O red. Reproduced with permission from ref 20a. Copyright 2015 Wiley-VCH. Local atomic structures around N in N-doped graphene. (b) Graphitic nitrogen near divacancy defect (DV-N). (c) Graphitic nitrogen near Stone−Wales (SW-N_2). (d) N-pair-doped Stone−Wales defect (SW-N_3N_3). The O_2 approaching C sites are labeled by numbers. Gray and blue balls denote carbon and nitrogen atoms, respectively. Reproduced with permission from ref 20b. Copyright 2014 American Chemical Society.

nitrogen atoms are located at edge and defect sites, and hence, these sites themselves can be highly active. An interconversion between the graphitic and pyridinic sites within a catalytic cycle has been proposed to reconcile the controversy whether the graphitic, pyridinic, or both nitrogen are active sites for ORR.[22] The correlation of nitrogen-binding configurations with electrocatalytic activity is of importance for designing efficient catalysts. A recent study revealed that the particular structure of a nitrogen-pair-doped Stone−Wales defect provided the best active site with a low overpotential for ORR in the volcano plot and that its ORR activity could be tuned by the curvature around the active site.[20b] In order to demonstrate the effect of nitrogen bonding state on the selectivity and catalytic activity for ORR, two different methods have been used to prepare N-doped graphene.[23] It was found that graphitic N and pyridinic N centers were preferentially formed by annealing of graphene oxide (GO) with ammonia, whereas annealing of polyaniline/reduced graphene oxide (RGO) and polypyrrole/RGO tended to generate pyridinic and pyrrolic N moieties, respectively. Generally speaking, the graphitic N content determines the limiting current density, whereas the pyridinic N content improves the onset potential for ORR.[23] Pyridinic-N can contribute one *p*-electron to the aromatic *p*-system and has a lone electron pair in the plane of carbon matrix, which can increase the electron-donating property of the catalyst. Thus, it would weaken the O−O bond via the bonding of oxygen with nitrogen and/or the adjacent carbon atom to facilitate the reduction of O_2. Nevertheless, the total N content in the nitrogen-doped RGO (NRGO) catalyst was demonstrated to not play an important role in the ORR process.

Along with the above mechanistic studies in the theoretical frontier, possible effects of metal residues on the ORR electrocatalytic activities have also been addressed experimentally to be nonexistent by demonstrating efficient ORR catalytic activities, even with a four-electron process, for various N-doped carbon-based ORR catalysts prepared via metal-free preparation procedures.[15,24,18a,25] Apart from those ORR catalysts prepared by metal-free syntheses reported earlier, heteroatom-doped graphitized nanodimands (NDs) with a high electrocatalytic activity have been recently prepared by laser irradiation of nongraphitized nanodiamonds, followed by doping with N and S atoms through thermal annealing under NH_3 and H_2S, respectively.[26] On the other hand, N-doped mesoporous carbons have also been achieved by carbonization of nucleobases dissolved in an ionic liquid at 1000 °C.[24c] Besides, metal-free N-doped carbons with a controllable pore texture have also been prepared by carbonization of ionic liquids,[27] leading to a four-electron pathway for ORR with an overpotential only slightly larger than that of the Pt/C electrode. In this particular case, both the ORR activity and kinetics were found to strongly correlate with the pore size distribution. More recently, various heteroatom-doped porous carbon structures have also been prepared by template-assisted syntheses from metal-free carbon precursors[12,27b,28] (e.g., polyaniline,[8a] triphenylphosphine,[29] and nitrogen-rich ionic liquids[24c]). In these cases, the pore structure of the resultant carbon-based catalysts can be tuned by using different templates, including ordered mesoporous silica, silica spheres, fermented rice, and triblock copolymer assemblies.[12] Furthermore, N-doped mesoporous carbon has been successfully prepared by pyrolysis of a nitrogen-containing aromatic dyestuff, *N*,*N*′-bis(2,6-diisopropyphenyl)-3,4,9,10-perylenetetracarboxylic diimide (PDI) onto a SBA-15 mesoporous silica template.[24a] The unique features of the porous graphitic carbon framework, together with its high surface area and moderate nitrogen content, led to high electrocatalytic activity toward ORR, excellent long-term stability, and high tolerance to crossover effect, which outperformed the commercially available Pt/C catalysts. Nitrogen-doped mesoporous carbon nanosheets have also been produced by a metal-free template approach.[30] The mesoporous carbon nanosheet catalysts with a pore size of ∼22 nm exhibited a comparable diffusion-limited current and more positive ORR onset potential than that of the Pt/C in alkaline medium. Because the unique planar porous structure could not only facilitate electrolyte/reactant diffusion but also provide abundant catalytic sites, good ORR catalytic performance with a long-term stability was observed even under acidic conditions. Along with the N-doping, Yang et al. extended the doping atoms to include boron with a lower electronegativity than that of carbon.[31] Their experimental results revealed that electron-deficient boron doping could also turn CNTs into active ORR catalysts with a positively shifted reduction potential and enhanced reduction current, as well as a good stability and high tolerance to methanol crossover and CO-poisoning effects. DFT calculations revealed that the relatively strong electronegativity of carbon with respect to boron led to the formation of positively charged boron atom favorable for chemisorption of O_2. In contrast, O_2 was adsorbed on the positively charged carbon atoms neighboring the nitrogen dopant in nitrogen-doped CNTs.[7] Thus, these experimental and theoretical results suggest that the doping-

DOI: 10.1021/acscatal.5b01563
ACS Catal. 2015, 5, 7244−7253

induced charge redistribution, regardless of whether the dopants have a higher (e.g., N) or lower (e.g., B) electronegativity than that of carbon, could create positively charged sites (C^+ or B^+) that are favorable for O_2 adsorption and subsequent reduction process.[32] For the pristine CNTs, this process could not have occurred as there is no charged site on the nanotube, and the ground state triplet O_2 would have repulsion force with spin-singlet pristine CNTs owing to orbital mismatch.[31]

As a building block for various carbon nanomaterials, including CNTs, graphene sheets have also been demonstrated to show a superb ORR performance after doping with nitrogen.[33] Theoretical calculations indicate that the edge defects of graphene can lower energy barriers for the oxygen adsorption and electron transfer significantly to achieve a direct four-electron pathway for ORR.[22,34] The active sites on a N-doped graphene sheet have been shown to be around carbon atoms with either high positive charge densities or high positive spin densities, indicating that N-doped carbons are inherently catalytic active.[34a] It is interesting to note that N-doped porous graphene has also been prepared as an efficient metal-free ORR electrocatalyst by generating nanopores in the graphene matrix, followed by nitrogen-doping along the pore openings.[35] Compared to N-doped nonporous graphene, the N-doped porous graphene displayed an excellent electrocatalytic activity toward ORR. This is presumably because the edge of graphene sheets was found to be more reactive than their basal plane.[31b,c] More interestingly, the electrocatalytic activity of N-doped graphene for ORR was found to change with the lateral size of graphene at the nanometer scale, as is the case with the N-doped graphene quantum dots (GQDs).[36] The larger GQDs with higher HOMO levels could be more easily oxidized, possibly leading to the higher catalytic activity. The size-dependent catalytic activity of the N-doped GQDs has important implications in understanding and further improving the catalytic activities of N-doped carbon nanomaterials. Besides, the effect of the N-doping sites (e.g., pyridinic-/graphitic-type) on the ORR activity in N-doped GQDs has been investigated.[37] First-principles calculations revealed that the pyridinic- and graphitic-type nitrogens are the dominant active sites in the N-doped nanocarbons for ORR. It is now possible to use a solution chemistry approach to not only control the numbers of nitrogen atoms in N-doped GQDs but also define their bonding configurations and hence the electrocatalytic activity.[38] Owing to the metal-free preparation procedures, the electrocatalytic activities observed with the aforementioned carbon-based ORR catalysts can be attributed exclusively to the incorporation of heteroatoms (e.g., N, B) into the graphitic carbon structures (i.e., heteroatom-doping). As can be seen from the above discussion, heteroatom-doping of graphitic carbons is an efficient approach for the development of carbon-based metal-free catalysts for oxygen reduction. Uncovering the underlying principle for the heteroatom-doped carbons as metal-free ORR catalysts is significant as the same principles can be applied for developing other metal-free catalysts for oxygen reduction and beyond ORR.[9c,39,36] Indeed, the basic principle has been used to develop a large variety of other heteroatom-doped (e.g., O, B, S, P, F, Cl, Br, I) carbon-based catalysts,[9b,29,40] as well as even certain polyelectrolyte-adsorbed all-carbon materials as efficient metal-free ORR catalysts.[41]

3. DOPED GRAPHITIC CARBON NANOSTRUCTURES BEYOND NITROGEN-DOPING

In addition to the aforementioned metal-free ORR catalysts based on carbons doped with nitrogen or boron with either a higher or lower electron electronegativity than that of carbon to induce charge transfer,[7,31] doping with sulfur (S) of a similar electronegativities as that of carbon (2.58 vs 2.55 for S vs C) was demonstrated to also cause a positive effect on the electrocatalytic activity of graphitic carbon materials toward ORR. As shown in Figure 3, S-doping graphene has been

Figure 3. Fabrication of sulfur-doped graphene by thermal exfoliation of graphite oxide prepared by the Staudenmaier, Hofmann, and Hummers method in CS_2, H_2S, or SO_2 atmospheres. Reproduced with permission from ref 42a. Copyright 2013 American Chemical Society.

achieved via the thermal exfoliation of graphite oxides in the presence of hydrogen sulfide, sulfur dioxide, or carbon disulfide, respectively.[42a] On the other hand, a dry ball-milling method was developed to produce efficient metal-free ORR electrocatalysts based on edge-selectively sulfurized graphene nanoplatelets (SGnPs) by milling graphite in the presence of sulfur (S_8).[42b] Subsequent oxidation of the SGnP into SOGnP further improved ORR activity. As revealed by theoretical calculations, the doping-induced spin density redistribution, rather than the charge redistribution, is responsible for the high ORR activity of SGnP and SOGnP.[42b] S-doped graphitic carbon electrocatalysts have also been prepared by other methods[43] from, for example, cycled lithium−sulfur batteries[44] and directly thermal annealing oxidized carbon nanotubes and *p*-benzenedithiol in nitrogen.[45]

Phosphorus is an element of the nitrogen group with the same number of valence electrons as nitrogen and often similar chemical properties.[46] Like boron, the electronegativity of P (2.19) is lower than that of C (2.55). Metal-free phosphorus-doped mesoporous carbons (POMCs) with different pore sizes have also been synthesized using SBA-15 mesoporous silica with different channel lengths as templates as well as triphenylphosphine and phenol as phosphorus and carbon sources, respectively.[29] The resultant phosphorus-doped porous

DOI: 10.1021/acscatal.5b01563
ACS Catal. 2015, 5, 7244−7253

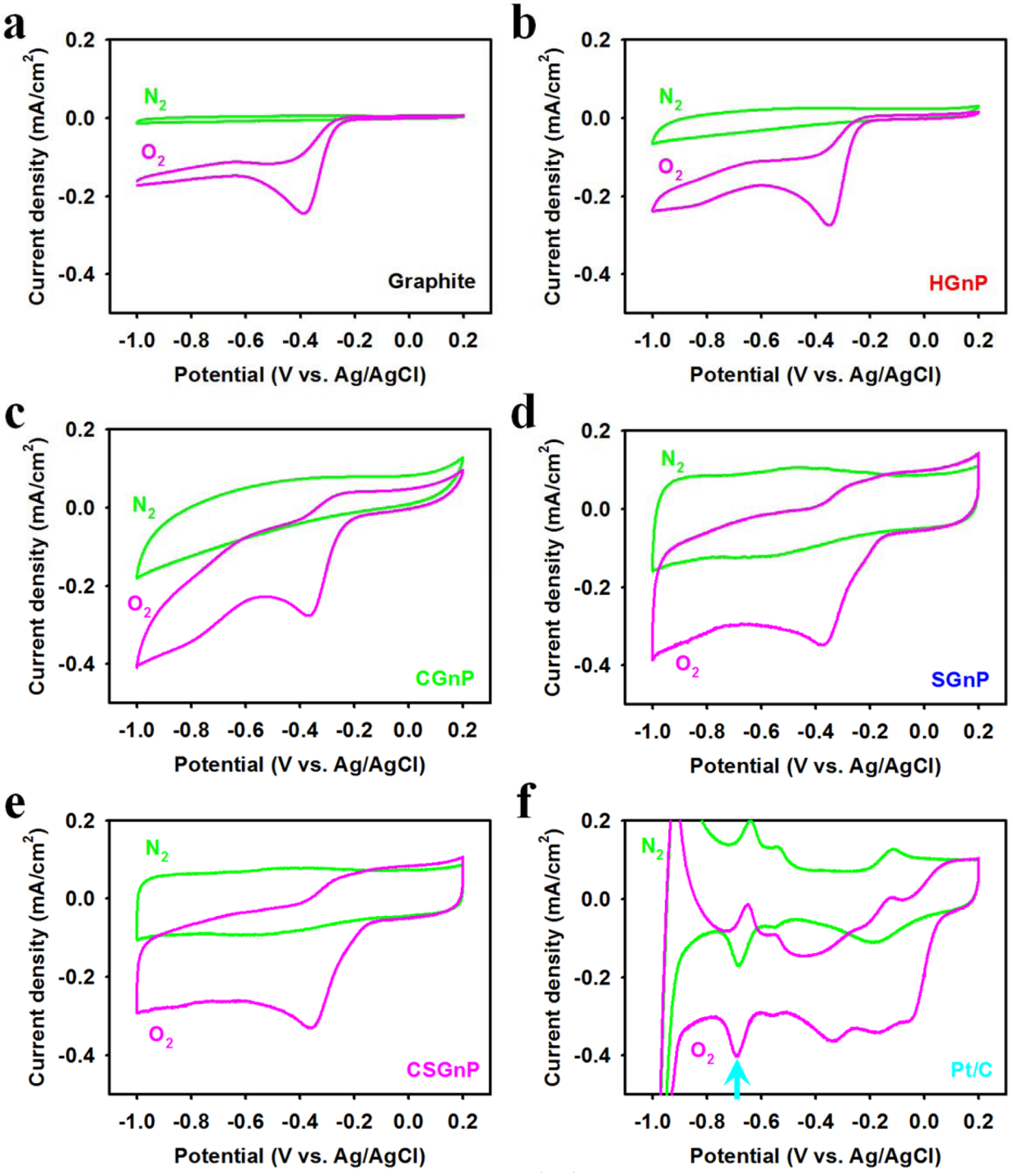

Figure 4. Cyclic voltammograms of sample electrodes on glassy carbon (GC) electrodes in N_2- and O_2-saturated 0.1 M aq KOH solution with a scan rate of 0.1 V/s: (a) pristine graphite; (b) HGnP; (c) CGnP; (d) SGnP; (e) CSGnP; (f) Pt/C. Reproduced with permission from ref 55. Copyright 2013 American Chemical Society.

carbon was demonstrated to exhibit an excellent electrocatalytic activity for a 4e ORR pathway in alkaline medium with enhanced stability and alcohol tolerance compared to those of Pt/C. P-doped graphene has also been prepared by thermal annealing of graphene oxide with P-containing precursors, such as 1-butyl-3-methylimidazoliumhexafluorophosphate, triphenylphosphine, P_4, and PH_3.[47] Besides, other heteroatoms, including halogen,[48] have also been used to dope graphitic carbons to enhance their catalytic activities.

Co-doping of graphitic carbons with more than one heteroatom has been demonstrated to potentially generate a synergic effect to enhance the catalytic activity toward ORR.[40c,49] Boron and nitrogen codoped graphene has been synthesized via thermal annealing of GO and boric acid composite in the atmosphere of ammonia,[40c] which has been shown to create a synergic effect for ORR. In order to eliminate the neutral effect and the formation of inactivated species, such as boron nitride (BN), the preparation process has to be modulated carefully.[50] A hierarchical micro/mesoporous

DOI: 10.1021/acscatal.5b01563
ACS Catal. 2015, 5, 7244−7253

Table 1. Electrocatalytic Performance of Heteroatom-Doped Metal-Free Carbons Obtained via Metal-Free Preparation Processes

method/precursor	electrocatalyst (mass loading, ug cm^{-2})	electrolyte	n[a]	on-set potential @ limiting current vs Pt/C[c]	fuel tolerance	ref
template method/PANi	N, O-doped mesoporous carbon (100)	0.1 M KOH	4	comparable@larger	-	8a
carbonization/nucleobases + ionic liquid	N-doped mesoporous carbon (800)	0.1 M KOH	4.1	comparable	CH_3OH	24c
spray pyrolysis/xylene + ethylenediamine	N-doped carbon spheres (286)	0.1 M KOH	3.86	comparable@smaller	CH_3OH	25a
template method/3-MBP-dca or CMIM-Cl[b]	N-doped hollow carbon hemisphere (~459)	0.1 M KOH	3.82	comparable@lower	CH_3OH	27b
template method/triphenylphosphine + phenol	P-doped mesoporous carbon[d]	0.1 M KOH	3.9	comparable	CH_3OH	29
electrochemical approach/graphene sheets	N-doped GQD (~286)	0.1 M KOH	3.6−4.4	smaller	CH_3OH	36a
solution chemistry approach	N-doped GQD (~77)	0.1 M KOH	3.9	smaller@lower		38
pyrolysis/carbon black + NH_4F	F-doped carbon black (400)	0.1 M KOH	3.9	better	CH_3OH and CO	48b
pyrolysis/carbon black + melamine ($C_3H_6N_6$) and ammonium fluoride (NH_4F)	N,F-codoped carbon (~510)	0.1 M KOH	4.2	comparable	CH_3OH and CO	54
template method/sucrose + thiourea	S,N codoped carbon foam (~143)	0.1 M KOH	3.96	comparable	CH_3OH	60a
pyrolysis/ethylenediamine + GO	g-C_3N_4/RGO nanosheet (~70.7)	0.1 M KOH	4.0	-	CH_3OH	60b
incorporation/g-C_3N_4 + mesoporous carbon	g-C_3N_4@carbon (84.8)	0.1 M KOH	4	lower	CH_3OH	60c
sputtting and annealing	N-doped carbon film[d]	0.1 M KOH	4	comparable	CH_3OH	60d
pyrolysis/gram flour	N-doped porous carbon (~255)	0.1 M KOH	4	comparable@smaller	CH_3OH	60e
pyrolysis/sugar and urea	N-doped graphene (283)	0.1 M KOH	4	comparable	CH_3OH	60f
thermal treatment/polypyridine + carbon black	N-doped carbon (~135)	0.1 M KOH	3.8	comparable	-	60g
carbonization/sucrose + 4-hydroxyphenylboronic acid	B-doped mesoporous carbon[d]	0.1 M KOH	4	lower@larger	CH_3OH and CO	60h
pyrolysis/carbohydrate-based derivatives and phenolic compound	N-doped carbon aerogels (~287)	0.1 M KOH	3.7	lower	CH_3OH	60i
pyrolysis/DNA + $CaCO_3$	N-doped mesoporous carbon (~200)	0.1 M KOH	4.02	lower@larger	-	60j
template method/(1-methyl-1H-pyrrole-2-yl) methanol	N-doped porous carbon (200)	0.5 M H_2SO_4	2	-	-	62
pyrolysis/pyromellitic acid dianhydride + 4,4′-oxidianilin	Fe-free N-doped carbon (40−300)	0.5 M H_2SO_4	2	lower@lower	-	63
C-ORNL-1 and NH_3	N-OMCs (~102)	0.05 M H_2SO_4	3.72	lower	CO	17
metal-free CVD of CH_4 and H_2	N-doped SWCNTs[d]	0.5 M H_2SO_4	>3.5	-	-	21a

[a]Electron transferred number for ORR. [b]3-Methyl-1-butylpyridine dicyanamide, 3-(3-cyanopropyl)-1-methyl-1*H*-imidazol-3-ium chloride. [c]The commercial Pt/C catalysts are commonly used as references: 20 wt % Pt on Vulcan X72R from ElectroChem, Inc., 20 wt % Pt on carbon black from Alfa Aesar. [d]The mass loading of electrocatalyst is not provided.

carbon foam codoped with N and S (NS-MC) has been prepared via thermal treatment of polyaniline coated sulfur sphere composite to exhibit excellent electrocatalytic activity with a high onset potential, large kinetic current density, high tolerance to methanol crossover effect, and long durability.[51] The dual doping of RGO with S and N has also been achieved by reducing GO in the presence of ethylene glycol and thiourea.[52] The resultant codoped RGO exhibited good catalytic activity for ORR via the favorable four-electron pathway due to a synergic effect between the N- and S-doping. Besides, nitrogen and phosphorus codoped RGO (NP-RGO) has been prepared by direct pyrolysis of a polymer gel composed of phytic acid, PANi, and/or GO, exhibiting superb bifunctional catalytic activity toward both ORR and OER with a low overpotential and large catalytic current density.[53]

By doping graphene with iodine and ammonia, I and N codoped graphene (ING) was prepared and used as metal-free catalyst for ORR both in alkaline and acidic media.[54] The as-prepared catalyst exhibited striking activity in alkaline with an onset potential of 0.945 V (vs RHE), which is the same as that of commercial Pt/C catalyst. Synergic effects have also been achieved for edge-codoped GnPs by ball-milling graphite in the presence of sulfur and dry ice and subsequent exposure to air moisture to produce GnP edge-functionalized (codoped) with −COOH and $-SO_3H$ (CSGnP).[55] Because the polarities of edge groups are in the order of $-SO_3H$ > −COOH > −H, the polarity order is expected to be SGnP > CSGnP > CGnP > HGnP > the pristine graphite. As can be seen in Figure 4, the overall electrocatalytic activities were found to be closely related to the edge polarity nature in the order of SGnP >

DOI: 10.1021/acscatal.5b01563
ACS Catal. 2015, 5, 7244−7253

CSGnP > CGnP > HGnP > the pristine graphite, indicating the effective tuning catalytic activities by edge-(co)doping.[55,56]

Table 1 lists various heteroatom-doped, carbon-based ORR catalysts generated by metal-free preparation procedures. Many of them exhibited efficient ORR catalytic activities with a 4e process, which clearly confirms that heteroatom-containing carbons are inherently catalytic active because no metal was used for the material preparation and subsequent doping in these cases.

In spite of the numerous previous studies that have clarified the originality of the catalytic activity for graphitic carbon ORR catalysts generated from either a metal-free preparation procedure or after careful removal of metal residues by postsynthesis purification,[28c,32,57] there are still some concerns of possible contributions of metal impurities to the ORR activities of metal-free catalysts.[11] In particular, Schuhmann and co-workers reported that the ORR activity of nitrogen-modified carbon catalysts could be promoted by the addition of trace metals (e.g., Fe, Co, Mn) for high-temperature annealing.[11a] On this basis, these authors concluded that trace metal residues promote the activity of metal-free carbon catalysts for oxygen reduction. However, the claim was made by igorning the electrocatalytic mechanism of metal-free ORR catalysts associated with heteroatom-doping-induced (e.g., N-doping) charge-transfer in graphitic carbon materials (vide supra). It is not a surprise to find that the ORR activity of carbon-based metal-free catalysts can be enhanced by the addition of trace metals as the importance of metallic species in the well-studied M−Nx−C type nonprecious metal catalysts (NPMCs, M = Fe, Co, or Ni) has been long recognized. Nevetheless, it is still a debate as to whether the metal is involved in constituting the active site in M−Nx−C catalysts or that it merely facilitates the formation of active sites under thermal treatment.[58,59] Wu et al. have recently prepared a new class of NPMCs via high-temperature synthesis of Fe- and Co-based catalysts in the presence of polyaniline (PANI), which showed high ORR performance with an excellent durability.[59] It was found that transition metal is indispensable to catalyze the graphitization of nitrogen−carbon precursor to form the highly graphitized carbon, including carbon tubes, onion-like carbon, and platelets (multilayer graphene), while nitrogen species embedded within the in situ formed graphitized carbon nanostructures are critical to the active-site performance. Generally speaking, graphitic carbon with a conjugated structure of alternating C−C single and C═C double bonds is a prerequisite for charge-transfer to occur upon the heteroatom-doping, and hence only graphitic (not amorphous) carbon materials with the conjugated structure could act as a metal-free ORR catalyst through the doping-induced charge-transfer. This important point is often misunderstood or ignored, as is the case with the ref 11a. Therefore, the presence of metal during the pyrolysis processes reported in refs 11a and 59 is, most probably, to facilitate the formation of graphitic carbon active sites. This is consistent with the fact that many efficient ORR catalysts based on various graphitic nanocarbon structures have been prepared by metal-free preparation procedures without the involvement of any metal-containing precursors throughout the entire synthesis processes (see Table 1).[8a,17,21a,24c,25a,27b,29,36a,38,48b,54,60,62,63] Recent theoretical studies have also clearly indicated that the N−C active centers in metal-free catalysts can directly reduce oxygen into H_2O via either a 4e process or a less effective 2e pathway without involving any metal.[34b,61]

In a similar study, Pumera and co-workers investigated the ORR catalytic activities of graphene materials produced by different preparation methods, including the Hummers[64] and Staudenmaier[65] methods by oxidizing graphite with permanganate oxidant and chlorate oxidant, respectively, followed by a chemical reduction with hydrazine to generate G-HU and G-ST graphene.[11b,66] These reduced graphene oxides (RGOs) prepared via these two different methods were demonstrated to contain different amounts of metal impurities (e.g., Mn, Fe, Co, Ni) and to show different onset potentials and oxygen reduction currents (Figure 5a). From the above observation made on undoped graphene, these authors claimed that ORR electrocatalysis of the heteroatom-doped graphene is caused by metallic impurities (e.g., MnO_2) present within the graphene materials. By performing a similar study on CNTs, the same authors have also made a recent claim that residual metallic

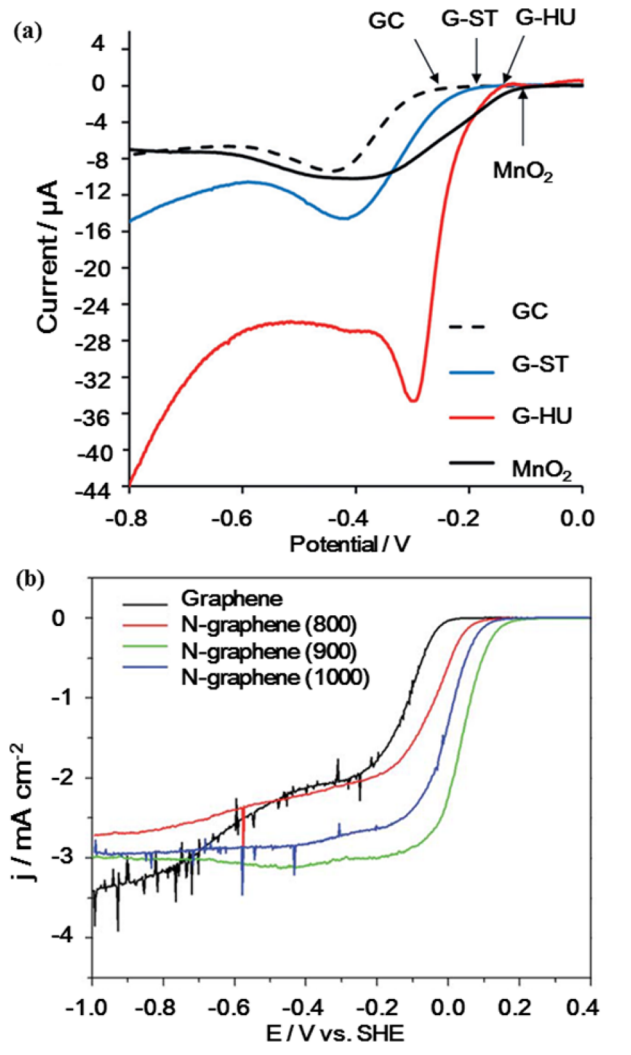

Figure 5. (a) Linear sweep voltammograms recorded in air-saturated 0.1 M KOH solution using a bare glassy carbon electrode (black-dashed line) and a GC electrode modified with G-HU (red line) and G-ST (blue line) graphene materials. Scan rate: 0.1 V s^{-1}. Reproduced with permission from ref 11b. Copyright 2013 Wiley VCH. (b) The linear-sweep voltammograms of graphene and N-graphene prepared under different temperatures. Electrolyte: O_2-saturated 0.1 M KOH. Scan rate: 5 mV s^{-1}. Rotation speed: 1600 rpm. Reproduced with permission from ref 68. Copyright 2011 The Royal Society of Chemistry.

DOI: 10.1021/acscatal.5b01563
ACS Catal. 2015, 5, 7244−7253

impurities are responsible for ORR activities in metal-free CNT catalysts.[11c] While the presence of MnO_2 was shown to enhance the ORR activity, iron, cobalt, and nickel oxides were found to not exhibit any significant electrocatalytic effect on the ORR. It is not a surprise that the RGOs obtained by different preparation methods exhibited different ORR activities as different oxidation methods could led to RGOs with different structures/defects[67] and hence different ORR behaviors.[11b,66a] Thus, cautions are needed in drawing conclusions by comparing materials prepared by different methods with different structures without comprehensive characterization. It has been widely recongnized that the ORR conducted on carbons without heteroatom-doping usually exhibits the two-step, 2e pathway (Scheme 1, Figure 5a) rather than the one-step, 4e pathway, as observed on the Pt/C, NCNT (curves 1 and 3 in Figure 1a) and N-doped graphene (Figure 5b).[68] Clearly, therefore, the intrinsic nonmetal active sites in N-doped carbons showed diffierent ORR behavior from that of the metal active centers, including the trace metal residues (Figure 5a). Recently, different behaviors toward electrocatalysis of ORR have also been observed for N-doped carbon catalysts and NPMCs even in PEMFCs.[69] In addition, more and more recently published papers report carbon-based metal-free catalysts for not only ORR but also OER, HER, and their combinations,[10] which simply cannot be explained by the trace metal residues as the trace metal residues, if any, could not have activities for all of these reactions, particularly as efficient bifunctional catalysts to catalyze two reactions simultaneously. Also, it is a well-known fact that metal active centers are suspectible to CO-poisioning, whereas carbon-based metal-free ORR catalysts are free from the CO-poisioning effect. This clearly indicates that the trace metal, if any, is not responsible for the observed ORR activities of the carbon-based metal-free catalysts. Furthermore, the observations that the physically absorbed positively charged metal-free polymers (e.g., PDDA) onto metal-free all-carbon graphene or all-carbon nanotubes caused an increase in the ORR activity through the intermolecular charge-transfer[41b] unambiguously indicate, once again, that it is the charge-transfer, rather than the trace metal, which is responsible for the ORR activities in the metal-free carbon-based catalysts. Through electrochemical measurements and DFT calculations, Qiao and co-workers have revealed the origin of electrocatalytic activity of heteroatom-doped graphene-based metal-free electrocatalysts for ORR.[70] A volcano plot (Figure 6) between the ORR activity and the adsorption free energy of intermediates on the heteroatom-doped graphene materials has been derived, predicting that the ORR catalytic activity of an ideal heteroatom-doped graphene metal-free catalyst is comparable to, or even better than, that of the Pt/C catalyst.[70]

Although heteroatom-doped carbon nanomaterials have been demonstrated to be intrinsically active metal-free catalysts for ORR, their catalytic performance in acidic media still needs to be further improved.[71] The low surface density of catalytic sites is believed to be one of the limiting factors for the poor performance in acids. However, nitrogen-doped ordered mesoporous carbons synthesized via NH_3 activation exhibited a significant ORR activity in acidic media with a better stability than a commercial Pt/C catalyst.[17] Nitrogen-doped graphene with a high yield of planar N (90.3%) showed good N incorporation, excellent electronic conductivity, and good catalytic activity toward the ORR even in acidic electrolytes.[72] More recently, a new class of carbon-based ORR catalysts that

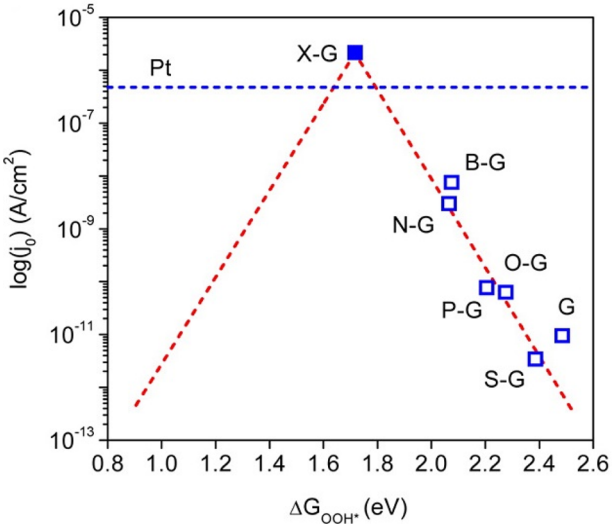

Figure 6. Important Volcano plot between j_0 theory and ΔG_{OOH^*} with charge-transfer coefficient α = 0.5 (red dashed line). Blue hollow squares are j_0^{expt} obtained from Tafel plots and DFT-derived ΔG_{OOH^*} for each doped graphene catalyst. Reproduced with permission from ref 70. Copyright 2014 American Chemical Society.

worked well in acid PEMFCs[69] has been developed by mixing N-doped graphene with acid-oxidized CNTs and carbon black particles in solution, followed by freeze-drying. In the resultant 3D porous carbon foams (N-G-CNT), N-graphene provided large surface area to speed ORR while nanotubes enhanced conductivity and carbon black separated the graphene sheets for free flow of the electrolyte and oxygen, leading to the improved ORR performance. The PEMFC with N-G-CNT catalyst exhibited a peak power density of 300 W g^{-1}, comparable to high-performance Fe(Co)/N/C catalysts.[69] More importantly, the metal-free catalyst showed an excellent operational durability with a relatively small current decay (~20% decay over 100 h) in PEMFCs operating at a constant voltage of 0.5 V with pure H_2/O_2 as fuel gases. In contrast, the Fe/N/C catalyst showed an initial sharp current decay with a total of about 75% decay over 100 h at both the high (2 mg cm^{-2}) and low loadings (0.5 mg cm^{-2}). This work clearly indicates that N-doped carbon nanomaterials are durable catalysts for ORR even in acidic fuel cells (e.g., PEMFCs) and opens possibilities for clean energy generation from affordable and durable PEMFCs based on low-cost, metal-free, carbon-based ORR catalysts.

4. SUMMARY AND OUTLOOK

As can be seen from above discussions, N-doped graphitic carbons, including carbon nanotubes, graphene, and porous carbons, have been demonstrated to show excellent electrocatalytic activities for ORR. The improved catalytic performance has been attributed to the N-doping-induced charge redistribution around the nitrogen dopants, which could lower the ORR potential and change the O_2 chemisorption mode to effectively weaken the O−O bonding, facilitating ORR at the metal-free N-doped nanocarbon electrodes. Uncovering this new ORR mechanism in the N-doped carbon catalysts is significant as the same principle has been applied to the development of various other efficient metal-free ORR catalysts based on heteroatom-doped (e.g., O, B, S, P, F, Cl, Br, I) carbons, certain polyelectrolyte-adsorbed all-carbon nanoma-

DOI: 10.1021/acscatal.5b01563
ACS Catal. 2015, 5, 7244−7253

terials (e.g., undoped CNTs, graphene), and even metal-free ORR/OER/HER bifunctional catalysts. Among them, many heteroatom-doped, carbon-based ORR catalysts were generated by metal-free preparation procedures (Table 1) to exhibit efficient ORR catalytic activities with a 4e process, clearly indicating that heteroatom-doped carbons are inherently catalytic active without the needs of any metal involvement. Although the field of metal-free carbon-based ORR catalysis is still very young with respect to NPMCs that have been extensively researched for decades, metal-free ORR catalysts have shown great potentials for practical applications even in PEMFCs. The use of heteroatom-doped carbon nanomaterials as metal-free ORR catalysts could dramatically reduce the cost and increase the efficiency of fuel cells. Before their large-scale practical applications in fuel cells can be realized, however, new combined experimental and theoretical approaches need to be developed to precisely determine the locations and structures of the active sites. In comparison with the well-established evolution and fabrication procedures for metal-based catalysts, physicochemical characterization of carbon-based metal-free electrocatalysts and fundamental understanding of their structure−property relationships are still under developed. Furthermore, a standard fabrication method needs to be developed for the fabrication of membrane electrode assemblies (MEAs) for performance testing of the metal-free electrocatalysts in practical fuel cells and/or metal−air batteries. Although much work still needs to be done, this is clearly an area in which future work would be of value. Continued research and development efforts in this exciting field will surely translate low-cost, metal-free, carbon-based ORR catalysts to commercial reality.

AUTHOR INFORMATION

Corresponding Author

*E-mail: liming.dai@case.edu.

Present Address

[†]Key Laboratory of Colloid and Interface Chemistry, Ministry of Education, School of Chemistry and Chemical Engineering, Shandong University, Jinan 250100, China

Notes

The authors declare no competing financial interest.

ACKNOWLEDGMENTS

The authors thank colleagues for their contributions to the work cited. We are also grateful for financial support from NSF (CMMI-1400274, CMMI-1266295, AIR-IIP-1343270, DMR 1106160) and DOD-AFOSR-MURI (FA9550-12-1-0037).

REFERENCES

(1) (a) Armand, M.; Tarascon, J. M. *Nature* **2008**, *451*, 652−657. (b) Katsounaros, I.; Cherevko, S.; Zeradjanin, A. R.; Mayrhofer, K. J. J. *Angew. Chem., Int. Ed.* **2014**, *53*, 102−121.

(2) Zhang, J.; Guo, C.; Zhang, L.; Li, C. M. *Chem. Commun.* **2013**, *49*, 6334−6336.

(3) Debe, M. K. *Nature* **2012**, *486*, 43−51.

(4) (a) Winther-Jensen, B.; MacFarlane, D. R. *Energy Environ. Sci.* **2011**, *4*, 2790−2798. (b) Rabis, A.; Rodriguez, P.; Schmidt, T. J. *ACS Catal.* **2012**, *2*, 864−890. (c) Winther-Jensen, B.; Winther-Jensen, O.; Forsyth, M.; MacFarlane, D. R. *Science* **2008**, *321*, 671−674.

(5) (a) Suntivich, J.; Gasteiger, H. A.; Yabuuchi, N.; Nakanishi, H.; Goodenough, J. B.; Shao-Horn, Y. *Nat. Chem.* **2011**, *3*, 546−550. (b) Lefèvre, M.; Proietti, E.; Jaouen, F.; Dodelet, J.-P. *Science* **2009**, *324*, 71−74.

(6) Gasteiger, H. A.; Marković, N. M. *Science* **2009**, *324*, 48−49.

(7) Gong, K.; Du, F.; Xia, Z.; Durstock, M.; Dai, L. *Science* **2009**, *323*, 760−764.

(8) (a) Silva, R.; Voiry, D.; Chhowalla, M.; Asefa, T. *J. Am. Chem. Soc.* **2013**, *135*, 7823−7826. (b) Dai, L.; Chang, D. W.; Baek, J.-B.; Lu, W. *Small* **2012**, *8*, 1130−1166. (c) Pandolfo, A. G.; Hollenkamp, A. F. *J. Power Sources* **2006**, *157*, 11−27. (d) Su, D. S.; Centi, G. *J. Energy Chem.* **2013**, *22*, 151−173.

(9) (a) Dai, L.; Xue, Y.; Qu, L.; Choi, H. J.; Baek, J. B. *Chem. Rev.* **2015**, *115*, 4823−4892. (b) Daems, N.; Sheng, X.; Vankelecom, I. F. J.; Pescarmona, P. P. *J. Mater. Chem. A* **2014**, *2*, 4085−4110. (c) Su, D. S.; Perathoner, S.; Centi, G. *Chem. Rev.* **2013**, *113*, 5782−5816. (d) Huang, C.; Li, C.; Shi, G. *Energy Environ. Sci.* **2012**, *5*, 8848−8868. (e) Liu, J.; Xue, Y.; Zhang, M.; Dai, L. *MRS Bull.* **2012**, *37*, 1265−1272. (f) Chen, H.; Sun, F.; Wang, J.; Li, W.; Qiao, W.; Ling, L.; Long, D. *J. Phys. Chem. C* **2013**, *117*, 8318−8328.

(10) (a) Liu, J.; Liu, Y.; Liu, N.; Han, Y.; Zhang, X.; Huang, H.; Lifshitz, Y.; Lee, S.-T.; Zhong, J.; Kang, Z. *Science* **2015**, *347*, 970−974. (b) Shui, J.; Du, F.; Xue, C.; Li, Q.; Dai, L. *ACS Nano* **2014**, *8*, 3015−3022. (c) Zheng, Y.; Jiao, Y.; Zhu, Y.; Li, L. H.; Han, Y.; Chen, Y.; Du, A.; Jaroniec, M.; Qiao, S. Z. *Nat. Commun.* **2014**, *5*, 3783. (d) Zhang, J.; Zhao, Z.; Xia, Z.; Dai, L. *Nat. Nanotechnol.* **2015**, *10*, 444−452.

(11) (a) Masa, J.; Zhao, A.; Xia, W.; Sun, Z.; Mei, B.; Muhler, M.; Schuhmann, W. *Electrochem. Commun.* **2013**, *34*, 113−116. (b) Wang, L.; Ambrosi, A.; Pumera, M. *Angew. Chem., Int. Ed.* **2013**, *52*, 13818−21. (c) Wang, L.; Pumera, M. *Chem. Commun.* **2014**, *50*, 12662−12664.

(12) Zhao, A.; Masa, J.; Schuhmann, W.; Xia, W. *J. Phys. Chem. C* **2013**, *117*, 24283−24291.

(13) (a) Yuasa, M.; Yamaguchi, A.; Itsuki, H.; Tanaka, K.; Yamamoto, M.; Oyaizu, K. *Chem. Mater.* **2005**, *17*, 4278−4281. (b) Bashyam, R.; Zelenay, P. *Nature* **2006**, *443*, 63−66. (c) Yuan, X.; Ding, X.-L.; Wang, C.-Y.; Ma, Z.-F. *Energy Environ. Sci.* **2013**, *6*, 1105−1124.

(14) Liu, Z.-W.; Peng, F.; Wang, H.-J.; Yu, H.; Zheng, W.-X.; Yang, J. *Angew. Chem.* **2011**, *123*, 3315−3319.

(15) Nabae, Y.; Kuang, Y.; Chokai, M.; Ichihara, T.; Isoda, A.; Hayakawa, T.; Aoki, T. *J. Mater. Chem. A* **2014**, *2*, 11561−11564.

(16) Zhao, Y.; Watanabe, K.; Hashimoto, K. *J. Am. Chem. Soc.* **2012**, *134*, 19528−19531.

(17) Wang, X.; Lee, J. S.; Zhu, Q.; Liu, J.; Wang, Y.; Dai, S. *Chem. Mater.* **2010**, *22*, 2178−2180.

(18) (a) Yu, D.; Nagelli, E.; Du, F.; Dai, L. *J. Phys. Chem. Lett.* **2010**, *1*, 2165−2173. (b) Yuan, W.; Li, J.; Xie, A.; Chen, P.; Li, S.; Shen, Y. *Electrochim. Acta* **2015**, *165*, 29−35.

(19) (a) Hu, X.; Wu, Y.; Li, H.; Zhang, Z. *J. Phys. Chem. C* **2010**, *114*, 9603−9607. (b) Ikeda, T.; Boero, M.; Huang, S.-F.; Terakura, K.; Oshima, M.; Ozaki, J.-i. *J. Phys. Chem. C* **2008**, *112*, 14706−14709.

(20) (a) Masa, J.; Xia, W.; Muhler, M.; Schuhmann, W. *Angew. Chem., Int. Ed.* **2015**, *54*, 10102−10120. (b) Chai, G.-L.; Hou, Z.; Shu, D.-J.; Ikeda, T.; Terakura, K. *J. Am. Chem. Soc.* **2014**, *136*, 13629−13640.

(21) (a) Yu, D.; Zhang, Q.; Dai, L. *J. Am. Chem. Soc.* **2010**, *132*, 15127−15129. (b) Su, D. S.; Zhang, J.; Frank, B.; Thomas, A.; Wang, X.; Paraknowitsch, J.; Schlögl, R. *ChemSusChem* **2010**, *3*, 169−180.

(22) Kim, H.; Lee, K.; Woo, S. I.; Jung, Y. *Phys. Chem. Chem. Phys.* **2011**, *13*, 17505−17510.

(23) Lai, L.; Potts, J. R.; Zhan, D.; Wang, L.; Poh, C. K.; Tang, C.; Gong, H.; Shen, Z.; Lin, J.; Ruoff, R. S. *Energy Environ. Sci.* **2012**, *5*, 7936−7942.

(24) (a) Liu, R.; Wu, D.; Feng, X.; Müllen, K. *Angew. Chem., Int. Ed.* **2010**, *49*, 2565−2569. (b) Liang, J.; Zheng, Y.; Chen, J.; Liu, J.; Hulicova-Jurcakova, D.; Jaroniec, M.; Qiao, S. Z. *Angew. Chem., Int. Ed.* **2012**, *51*, 3892−3896. (c) Yang, W.; Fellinger, T.-P.; Antonietti, M. *J. Am. Chem. Soc.* **2010**, *133*, 206−209.

(25) (a) Zhou, X.; Yang, Z.; Nie, H.; Yao, Z.; Zhang, L.; Huang, S. *J. Power Sources* **2011**, *196*, 9970−9974. (b) Lyth, S. M.; Nabae, Y.; Moriya, S.; Kuroki, S.; Kakimoto, M.-a.; Ozaki, J.-i.; Miyata, S. *J. Phys. Chem. C* **2009**, *113*, 20148−20151.

DOI: 10.1021/acscatal.5b01563
ACS Catal. 2015, 5, 7244−7253

(26) Jang, D. M.; Im, H. S.; Back, S. H.; Park, K.; Lim, Y. R.; Jung, C. S.; Park, J.; Lee, M. *Phys. Chem. Chem. Phys.* **2014**, *16*, 2411−2416.
(27) (a) Zhang, Z.; Veith, G. M.; Brown, G. M.; Fulvio, P. F.; Hillesheim, P. C.; Dai, S.; Overbury, S. H. *Chem. Commun.* **2014**, *50*, 1469−1471. (b) Han, C.; Wang, J.; Gong, Y.; Xu, X.; Li, H.; Wang, Y. *J. Mater. Chem. A* **2014**, *2*, 605−609.
(28) (a) Maldonado, S.; Stevenson, K. J. *J. Phys. Chem. B* **2005**, *109*, 4707−4716. (b) Ai, K.; Liu, Y.; Ruan, C.; Lu, L.; Lu, G. *Adv. Mater.* **2013**, *25*, 998−1003. (c) Zheng, Y.; Jiao, Y.; Jaroniec, M.; Jin, Y.; Qiao, S. Z. *Small* **2012**, *8*, 3550−3566. (d) Sharifi, T.; Hu, G.; Jia, X.; Wågberg, T. *ACS Nano* **2012**, *6*, 8904−8912. (e) Tuci, G.; Zafferoni, C.; D'Ambrosio, P.; Caporali, S.; Ceppatelli, M.; Rossin, A.; Tsoufis, T.; Innocenti, M.; Giambastiani, G. *ACS Catal.* **2013**, *3*, 2108−2111. (f) Park, M.; Lee, T.; Kim, B.-S. *Nanoscale* **2013**, *5*, 12255−12260.
(29) Yang, D.-S.; Bhattacharjya, D.; Inamdar, S.; Park, J.; Yu, J.-S. *J. Am. Chem. Soc.* **2012**, *134*, 16127−16130.
(30) Wei, W.; Liang, H.; Parvez, K.; Zhuang, X.; Feng, X.; Müllen, K. *Angew. Chem., Int. Ed.* **2014**, *53*, 1570−1574.
(31) (a) Yang, L.; Jiang, S.; Zhao, Y.; Zhu, L.; Chen, S.; Wang, X.; Wu, Q.; Ma, J.; Ma, Y.; Hu, Z. *Angew. Chem., Int. Ed.* **2011**, *50*, 7132−7135. (b) Yuan, W.; Zhou, Y.; Li, Y.; Li, C.; Peng, H.; Zhang, J.; Liu, Z.; Dai, L.; Shi, G. *Sci. Rep.* **2013**, *3*, 2248. (c) Shen, A.; Zou, Y.; Wang, Q.; Dryfe, R.; Huang, X.; Dou, S.; Dai, L.; Wang, S. *Angew. Chem., Int. Ed.* **2014**, *53*, 10804−10808.
(32) Zhang, M.; Dai, L. *Nano Energy* **2012**, *1*, 514−517.
(33) Qu, L.; Liu, Y.; Baek, J.-B.; Dai, L. *ACS Nano* **2010**, *4*, 1321−1326.
(34) (a) Zhang, L.; Xia, Z. *J. Phys. Chem. C* **2011**, *115*, 11170−11176. (b) Zhang, L.; Niu, J.; Dai, L.; Xia, Z. *Langmuir* **2012**, *28*, 7542−7550.
(35) Palaniselvam, T.; Valappil, M. O.; Illathvalappil, R.; Kurungot, S. *Energy Environ. Sci.* **2014**, *7*, 1059−1067.
(36) (a) Li, Y.; Zhao, Y.; Cheng, H.; Hu, Y.; Shi, G.; Dai, L.; Qu, L. *J. Am. Chem. Soc.* **2011**, *134*, 15−18. (b) Li, Q.; Noffke, B. W.; Wang, Y.; Menezes, B.; Peters, D. G.; Raghavachari, K.; Li, L.-S. *J. Am. Chem. Soc.* **2014**, *136*, 3358−3361.
(37) Saidi, W. A. *J. Phys. Chem. Lett.* **2013**, *4*, 4160−4165.
(38) Li, Q.; Zhang, S.; Dai, L.; Li, L.-S. *J. Am. Chem. Soc.* **2012**, *134*, 18932−18935.
(39) (a) Xue, Y.; Liu, J.; Chen, H.; Wang, R.; Li, D.; Qu, J.; Dai, L. *Angew. Chem., Int. Ed.* **2012**, *51*, 12124−12127. (b) Feng, L.; Yan, Y.; Chen, Y.; Wang, L. *Energy Environ. Sci.* **2011**, *4*, 1892−1899.
(40) (a) Yang, Z.; Yao, Z.; Li, G.; Fang, G.; Nie, H.; Liu, Z.; Zhou, X.; Chen, X. a.; Huang, S. *ACS Nano* **2011**, *6*, 205−211. (b) Yang, S.; Zhi, L.; Tang, K.; Feng, X.; Maier, J.; Müllen, K. *Adv. Funct. Mater.* **2012**, *22*, 3634−3640. (c) Wang, S.; Zhang, L.; Xia, Z.; Roy, A.; Chang, D. W.; Baek, J. B.; Dai, L. *Angew. Chem., Int. Ed.* **2012**, *51*, 4209−4212.
(41) (a) Paraknowitsch, J. P.; Thomas, A. *Energy Environ. Sci.* **2013**, *6*, 2839−2855. (b) Wang, S.; Yu, D.; Dai, L. *J. Am. Chem. Soc.* **2011**, *133*, 5182−5185.
(42) (a) Poh, H. L.; Šimek, P.; Sofer, Z.; Pumera, M. *ACS Nano* **2013**, *7*, 5262−5272. (b) Jeon, I.-Y.; Zhang, S.; Zhang, L.; Choi, H.-J.; Seo, J.-M.; Xia, Z.; Dai, L.; Baek, J.-B. *Adv. Mater.* **2013**, *25*, 6138−6145.
(43) Duan, J.; Chen, S.; Jaroniec, M.; Qiao, S. Z. *ACS Catal.* **2015**, *5*, 5207−5234.
(44) Ma, Z.; Dou, S.; Shen, A.; Tao, L.; Dai, L.; Wang, S. *Angew. Chem.* **2015**, *127*, 1908−1912.
(45) Li, W.; Yang, D.; Chen, H.; Gao, Y.; Li, H. *Electrochim. Acta* **2015**, *165*, 191−197.
(46) Kong, X.; Chen, Q.; Sun, Z. *ChemPhysChem* **2013**, *14*, 514−519.
(47) (a) Li, R.; Wei, Z.; Gou, X.; Xu, W. *RSC Adv.* **2013**, *3*, 9978−9984. (b) Zhang, C.; Mahmood, N.; Yin, H.; Liu, F.; Hou, Y. *Adv. Mater.* **2013**, *25*, 4932−4937.
(48) (a) Yao, Z.; Nie, H.; Yang, Z.; Zhou, X.; Liu, Z.; Huang, S. *Chem. Commun.* **2012**, *48*, 1027−1029. (b) Sun, X.; Zhang, Y.; Song, P.; Pan, J.; Zhuang, L.; Xu, W.; Xing, W. *ACS Catal.* **2013**, *3*, 1726−1729.
(49) (a) Wang, S.; Iyyamperumal, E.; Roy, A.; Xue, Y.; Yu, D.; Dai, L. *Angew. Chem., Int. Ed.* **2011**, *50*, 11756−11760. (b) Domínguez, C.; Pérez-Alonso, F. J.; Al-Thabaiti, S. A.; Basahel, S. N.; Obaid, A. Y.; Alyoubi, A. O.; Gómez de la Fuente, J. L.; Rojas, S. *Electrochim. Acta* **2015**, *157*, 158−165. (c) Chen, J.; Zhang, H.; Liu, P.; Li, Y.; Li, G.; An, T.; Zhao, H. *Carbon* **2015**, *92*, 339−347.
(50) Liang, J.; Jiao, Y.; Jaroniec, M.; Qiao, S. Z. *Angew. Chem., Int. Ed.* **2012**, *51*, 11496−11500.
(51) Jiang, S.; Sun, Y.; Dai, H.; Hu, J.; Ni, P.; Wang, Y.; Li, Z. *Electrochim. Acta* **2015**, *174*, 826−836.
(52) Bag, S.; Mondal, B.; Das, A. K.; Raj, C. R. *Electrochim. Acta* **2015**, *163*, 16−23.
(53) Li, R.; Wei, Z.; Gou, X. *ACS Catal.* **2015**, *5*, 4133−4142.
(54) Zhan, Y.; Huang, J.; Lin, Z.; Yu, X.; Zeng, D.; Zhang, X.; Xie, F.; Zhang, W.; Chen, J.; Meng, H. *Carbon* **2015**, *95*, 930−939.
(55) Jeon, I.-Y.; Choi, H.-J.; Jung, S.-M.; Seo, J.-M.; Kim, M.-J.; Dai, L.; Baek, J.-B. *J. Am. Chem. Soc.* **2013**, *135*, 1386−1393.
(56) Dai, L. *Acc. Chem. Res.* **2013**, *46*, 31−42.
(57) Liang, H.-W.; Zhuang, X.; Brüller, S.; Feng, X.; Müllen, K. *Nat. Commun.* **2014**, *5*, 4973.
(58) (a) Dodelet, J.-P. In *Electrocatalysis in Fuel Cells*; Shao, M., Ed.; Springer: London, 2013; Vol. *9*, pp 271−338. (b) Xiang, Z.; Cao, D.; Huang, L.; Shui, J.; Wang, M.; Dai, L. *Adv. Mater.* **2014**, *26*, 3315−3320.
(59) Wu, G.; More, K. L.; Johnston, C. M.; Zelenay, P. *Science* **2011**, *332*, 443−447.
(60) (a) Liu, Z.; Nie, H.; Yang, Z.; Zhang, J.; Jin, Z.; Lu, Y.; Xiao, Z.; Huang, S. *Nanoscale* **2013**, *5*, 3283−3288. (b) Yang, S.; Feng, X.; Wang, X.; Müllen, K. *Angew. Chem., Int. Ed.* **2011**, *50*, 5339−5343. (c) Zheng, Y.; Jiao, Y.; Chen, J.; Liu, J.; Liang, J.; Du, A.; Zhang, W.; Zhu, Z.; Smith, S. C.; Jaroniec, M.; Lu, G. Q.; Qiao, S. Z. *J. Am. Chem. Soc.* **2011**, *133*, 20116−20119. (d) Chen, J.; Wang, X.; Cui, X.; Yang, G.; Zheng, W. *Chem. Commun.* **2014**, *50*, 557−559. (e) Gokhale, R.; Unni, S. M.; Puthusseri, D.; Kurungot, S.; Ogale, S. *Phys. Chem. Chem. Phys.* **2014**, *16*, 4251−4259. (f) Pan, F.; Jin, J.; Fu, X.; Liu, Q.; Zhang, J. *ACS Appl. Mater. Interfaces* **2013**, *5*, 11108−11114. (g) Xia, W.; Masa, J.; Bron, M.; Schuhmann, W.; Muhler, M. *Electrochem. Commun.* **2011**, *13*, 593−596. (h) Bo, X.; Guo, L. *Phys. Chem. Chem. Phys.* **2013**, *15*, 2459−2465. (i) Brun, N.; Wohlgemuth, S. A.; Osiceanu, P.; Titirici, M. M. *Green Chem.* **2013**, *15*, 2514−2524. (j) Wang, H.; Bo, X.; Luhana, C.; Guo, L. *Electrochem. Commun.* **2012**, *21*, 5−8.
(61) Yu, L.; Pan, X.; Cao, X.; Hu, P.; Bao, X. *J. Catal.* **2011**, *282*, 183−190.
(62) Park, J.; Nabae, Y.; Hayakawa, T.; Kakimoto, M.-a. *ACS Catal.* **2014**, *4*, 3749−3754.
(63) Muthukrishnan, A.; Nabae, Y.; Okajima, T.; Ohsaka, T. *ACS Catal.* **2015**, *5*, 5194−5202.
(64) Hummers, W. S.; Offeman, R. E. *J. Am. Chem. Soc.* **1958**, *80*, 1339−1339.
(65) Staudenmaier, L. *Ber. Dtsch. Chem. Ges.* **1898**, *31*, 1481−1487.
(66) (a) Wong, C. H. A.; Sofer, Z.; Kubešová, M.; Kučera, J.; Matějková, S.; Pumera, M. *Proc. Natl. Acad. Sci. U. S. A.* **2014**, *111*, 13774−13779. (b) Chua, C. K.; Ambrosi, A.; Sofer, Z.; Macková, A.; Havránek, V.; Tomandl, I.; Pumera, M. *Chem. - Eur. J.* **2014**, *20*, 15760−15767.
(67) (a) Chua, C. K.; Pumera, M. *Chem. Soc. Rev.* **2014**, *43*, 291−312. (b) Dreyer, D. R.; Park, S.; Bielawski, C. W.; Ruoff, R. S. *Chem. Soc. Rev.* **2010**, *39*, 228−240.
(68) Geng, D.; Chen, Y.; Chen, Y.; Li, Y.; Li, R.; Sun, X.; Ye, S.; Knights, S. *Energy Environ. Sci.* **2011**, *4*, 760−764.
(69) Shui, J.; Wang, M.; Du, F.; Dai, L. *Sci. Adv.* **2015**, *1*, e1400129.
(70) Jiao, Y.; Zheng, Y.; Jaroniec, M.; Qiao, S. Z. *J. Am. Chem. Soc.* **2014**, *136*, 4394−403.
(71) (a) Mo, Z.; Liao, S.; Zheng, Y.; Fu, Z. *Carbon* **2012**, *50*, 2620−2627. (b) Shi, Q.; Peng, F.; Liao, S.; Wang, H.; Yu, H.; Liu, Z.; Zhang, B.; Su, D. *J. Mater. Chem. A* **2013**, *1*, 14853−14857.
(72) Ding, W.; Wei, Z.; Chen, S.; Qi, X.; Yang, T.; Hu, J.; Wang, D.; Wan, L.-J.; Alvi, S. F.; Li, L. *Angew. Chem., Int. Ed.* **2013**, *52*, 11755−11759.

DOI: 10.1021/acscatal.5b01563
ACS Catal. 2015, 5, 7244−7253